62. Angular Distortions at Tetracoordinate Carbon

Planoid Distortions in α,α′-Bridged Spiro[4.4]nonanes and [5.5.5.5]Fenestranes

by **Wolfgang Luef** and **Reinhart Keese***

Institut für organische Chemie der Universität, Freiestrasse 3, CH-3012 Bern

Dedicated to Professor *Albert Eschenmoser*

(24.II.87)

Structures of α,α′-bridged spiro[4.4]nonanes and [5.5.5.5]fenestranes, obtained from X-ray analysis and MNDO calculations, are investigated in terms of symmetry-deformation coordinates. The central $C(C)_4$ fragments of these molecules show strong preference for compression, which is due to opening of opposite bond angles. The planoid deformations and strain energies of the fenestranes are discussed.

It has been recognized that the configuration of the spiro centre in annulenes with a central C-atom and in unsaturated as well as saturated fenestranes show planoid distortions [1–3]. In [4], such displacements have been discussed in terms of symmetry-deformation coordinates. For crystal structures of polycyclic molecules containing spiro-[4.4]nonane subunits with α,β′- or β,β′-polymethylene bridges, it has been shown, that the planoid distortions in the central $C(C)_4$ fragment of these molecules are due to closing of the two opposite intra-ring bond angles and to twist. In this paper, planoid distortions in the central $C(C)_4$ fragment of spiro[4.4]nonanes with one or two C bridges in the α,α′-positions between the two rings will be discussed (*Fig. 1*, **I** and **II**)[1]). As before [4], the planarizing deformations in the central $C(C)_4$ fragment of these tri- and tetracyclic compounds are related to the principal C_2 axis, which in these cases bisects the bond angles θ_{12} and θ_{34} (*Fig. 1*). To assess these deformations, crystal structures as well as MNDO results of these spiro molecules are considered. The spiroalkanes of type **I** and **II**

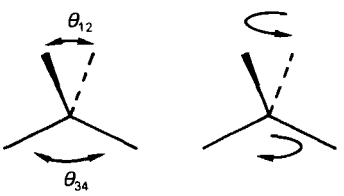

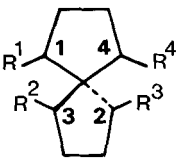

I $R^1 + R^2 = -(CH_2)_m-$, $R^3 = R^4 = H$, $m = 0, 1, 2$

II $R^1 + R^2 = -(CH_2)_m-$, $R^3 + R^4 = -(CH_2)_n-$, $m = 2$, $n \geq 2$

Fig. 1. *Compression* (S_{2a}) *and twist deformation* (S_{2b}) *of the* $C(C)_4$ *fragment of* **I** *and* **II**

[1]) For definitions, see [4].

(Fig. 1) constitute that subclass of centropolyquinanes that has conserved twofold symmetry [5][2]).

Data Selection. – The *Cambridge Structural Data Base* (updated version of June 1985 with 42 145 entries [7]) was searched for structures containing spiro[4.4]nonane subunits. From the 81 entries found those with $R < 0.1$ and polymethylene bridges between one or both α,α'-positions of the two spiro rings were selected. With the exception of **3** and **5** (where $\sigma(C-C_{av}) \leq 0.06$ Å), all structures with $\sigma(C-C_{av}) > 0.03$ Å were rejected. For the resulting 21 molecules containing 27 spiro[4.4]nonane subunits, bond angles and bond lengths were taken as obtained. For fenestranes, crystal-structure data and MNDO results [8] were used *(Appendix)*.

Discussion. – It is apparent from the crystal and MNDO structures of the spiro[4.4]nonanes of type **I** and **II** *(Fig. 1)*, that the central $C(C)_4$ fragments display, in most cases, bond-angle deformations with dominant if not exclusive $S_2(E)$ character *(Fig. 2)*. This is comparable to the results in [4] and indicates that planoid distortions are also dominant in spiro[4.4]nonanes, which are bridged in α,α'-positions. Examples of spiro structures of type **I** *(Fig. 1)* are found amongst natural products like the sesterterpene retigeranic acid (**1b**), isocomenediol (**2**), the tetracyclic molecule **3**, a derivative of ophiobolin D, and the synthetic pentacyclic molecule **4**. Although the chain connecting the spiro rings contains a N-atom, the derivative **5** of methyl secodaphniphyllate **6**, a degradation product of the diterpene alcaloid lycotomine, should be mentioned here. In **7**, the two rings of the spiro[4.4]nonane subunit again are connected by one ethylene bridge. The additional carbocyclic skeleton annellated in a special way induces, however, a dominant $S_4(T_2)$ deformation. Further examples of compounds, in which $s_4(T_2) > s_2(E)$ are **8** and **9**.

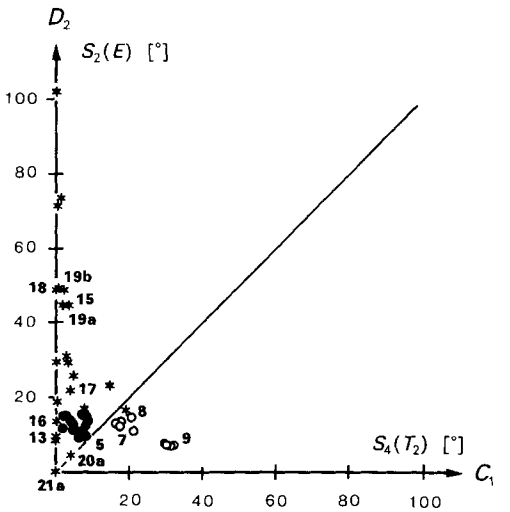

Fig. 2. $s_2(E)$ vs. $s_4(T_2)$ *bond-angle deformation vectors* [°] *for the central* $C(C)_4$ *fragment in substituted spiro[4.4]-nonanes of type* **I** *(Fig. 1)*. ●: crystal structure data; ○: structures with $s_2(E) < s_4(T_2)$; *: MNDO data.

[2]) Spiro structures with three-, four-, and five-membered rings and polymethylene bridges in one or both α,α'-positions including [4.4.5.5]- and [4.5.5.5]fenestranes will be discussed in [6].

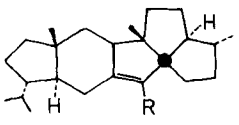

1a R = CONH(*p*-C_6H_4Br)
b R = COOH

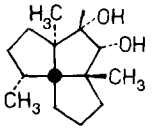

2

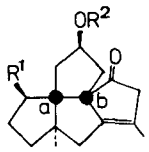

3 R^1 = $CH(CH_3)-(CH_2)_3-CH(CH_3)_2$
R^2 = SO_2(*p*-C_6H_4Br)

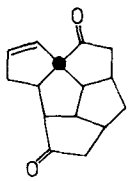

4

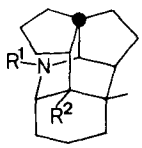

5 R^1 = $COCH_2Br$
R^2 = $(CH_2)_2COOCH_3$

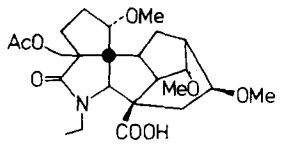

6

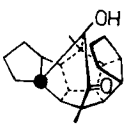

7

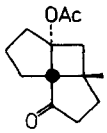

8

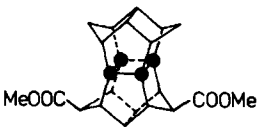

9

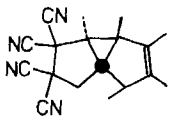

10

In the tricyclic molecule **8**, the distortion is intermediate between one conserving C_{2v}[3]) and D_2 symmetry ($s_2(E)$ = 14.43°, $s_4(T_2)$ = 21.33°). The dominant contribution from $S_4(T_2)$ to the overall distortion is due to the CH_2 bridge between the spiro rings which gives rise to a small angle in the cyclobutane ring (C(2)–C–C(4) = 88.8°) and a large opposite angle (C(1)–C–C(3) = 119.4°; C-numbering according to *Fig. 1*). The intra-ring bond angles in the spiro subunits of **8** differ only slightly, but are smaller than 109.47° (C(1)–C–C(4) = 106.6°, C(2)–C–C(3) = 105.2°). Similarly, the large $s_4(T_2)$ deformation vector in pagodane-dicarboxylate **9** is due to a considerable contribution from C_{2v}-type distortions, caused by the cyclobutane ring. This leads to four bond-angle situations comparable to the one found in **8**. Although its *R* factor > 0.1, the spiro structure **10** may be mentioned here. The direct C–C bond between the two spiro rings leads to an even larger $s_4(T_2)$ bond-angle deformation vector ($s_4(T_2)$ = 41.48°, $s_2(E)$ = 29.49°). This is characteristic of a structural entity with dominating C_{2v}-type distortions, which are caused by the large bond-angle deformations prevalent in cyclopropanes. The size of the bond angles at the spiro C-atom of the cyclopropyl ring (61.9°) and its external counterpart (120.4°) corroborates this interpretation.

The $s_2(E)$ deformations were further analyzed with respect to the $s_{2a}(E)$ and $s_{2b}(E)$ contributions *(Fig. 3)*. The $C(C)_4$ fragments of these α,α'-bridged spiro[4.4]nonanes differ from those with polymethylene bridges in α,β'- or β,β'-position [4] as their deformation vectors, related to the principal axis *(cf. Fig. 1)*, $s_{2a}(E)$ are > 0. Also, the $s_{2a}(E)$

[3]) In principle, C_1, C_s, C_{2v}, and C_{3v} symmetry is conserved under $S_4(T_2)$ deformations.

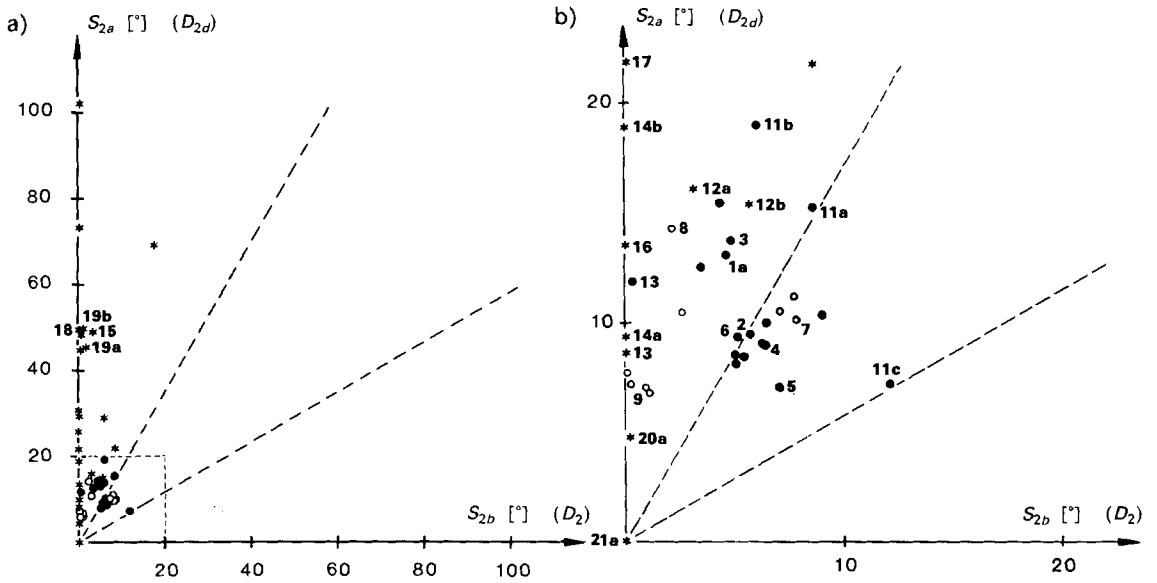

Fig. 3. *Bond-angle deformations* $S_{2a}(E)$ vs. $S_{2b}(E)$ *for the spiro centre in substituted spiro[4.4]nonanes of type* **I** (*Fig. 1*). a) Range of S_{2a} and S_{2b} 100°, b) Section of 20°. *: MNDO Data; ●: crystal structure data; ○: structures with $s_2(E) < s_4(T_2)$ (*cf. Fig. 2*).

vectors is variable in a larger range than the $s_{2b}(E)$-type deformation. Thus, one bridge between the α,α′-positions of the spiro rings may lead to considerable opening of opposite bond angle in the spiro[4.4]nonane substructures.

Typical examples are given by **1a** ($s_{2a} = 12.99°$, $s_{2b} = 4.5°$), a derivative of retigeranic acid **1b** and isocomenediol (**2**; $s_{2a} = 9.39°$, $s_{2b} = 5.55°$). Comparison of the S_{2a}/S_{2b}-type deformations around the spiro centre in **3** and **4** reveals that bridgehead double bonds in bridged spiro molecules of type **I** can affect the planoid deformation considerably. Whereas the spiro fragment *a* in **3** has s_{2a}/s_{2b} deformation vectors ($s_{2a} = 8.15°$, $s_{2b} = 5.04°$) very similar to that found in molecule **4** (as well as in **1** and **2**), the intra-ring angles in the spiro[4.4]nonane subunit *b* of **3** are opened up, leading to a larger S_{2a}-type deformation ($s_{2a} = 13.73°$, $s_{2b} = 4.798°$).

It is apparent from *Fig. 3b*, that the S_{2a}/S_{2b}-type distortions in all spiro molecules of type **I** and **II** are smaller than 20°. The S_{2a}-type distortions are larger than the S_{2b} (twist) deformations in most structures. In spiro structures with dominant $S_4(T_2)$ bond-angle deformations and a minor contribution from $S_2(E)$ distortions, compression ($s_{2a}(E)$) is larger than twist ($s_{2b}(E)$; *Fig. 3b*). X-Ray-structure analysis of spiro[4.4]nonanes with two polymethylene bridges connecting both α,α′-positions of the spiro rings have only been reported for the 7,7- and 6,6-vespirenes **11** and the fenestranes **12** and **13**. It is apparent from *Fig. 2* that the central $C(C)_4$ fragments of these molecules have bond-angle distortions with dominant $S_2(E)$ character. Comparison of the vespirenes **11a** and **11b** with the spirobifluorene **11c**, which contains one large bridge, reveals that the increasing planoid distortion is due to a growing contribution form compression ($S_{2a}(E)$; *Fig. 3*).

Fenestranes with a spiro[4.4]nonane skeleton can be considered as contracted vespirenes. Apart from the annulation with Ph rings, the vespirenes **11a** and **11b** contain a

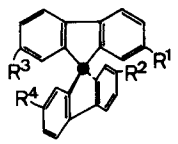

11a $R^1 + R^2 = R^3 + R^4 = -(CH_2)_7-$
b $R^1 + R^2 = R^3 + R^4 = -(CH_2)_6-$
c $R^1 + R^2 = -(CH_2OCH_2)_5-$, $R^3 = R^4 = H$

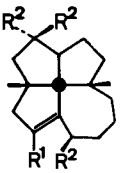

12a $R^1 = Br$, $R^2 = CH_3$
b $R^1 = R^2 = H$

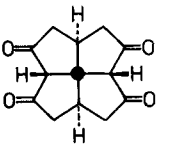

13

spiro[4.4]nonane ring system with the polymethylene bridges in both α,α′ -positions being longer than in the fenestranes. The shortening of both polymethylene bridges leads to large contribution from compression to the overall planoid distortion: in the tetraketone **13**, a derivative of [5.5.5.5]fenestrane (**14a**), the planoid deformation is essentially due to $S_{2a}(E)$-type distortion, whereas twist is lacking[4]).

MNDO Structures of [5.5.5.5]Fenestranes[5]). – Since the structural features of the molecules **12a**, **13**, and similar structures[6]) are well reproduced by MNDO calculations, it was of great interest to explore planoid distortion in fenestranes of type **II** (*Fig. 1*, $m = n = 2$) for which crystal structures have not been obtained. It is apparent from *Fig. 3* (*cf.* also *Appendix*) that the fenestranes investigated by MNDO calculations have bond angle distortions strongly dominated by compression ($s_{2a} \gg s_{2b}$). Particularly noteworthy are the stereoisomers of the [5.5.5.5]fenestrane[7])[8]). With an increasing number of *trans*-

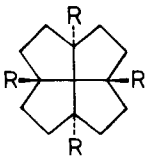

14a R = H
b R = CH_3

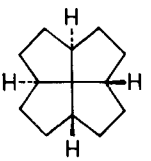

15

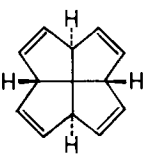

16

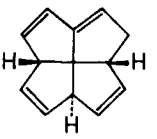

17

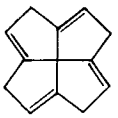

18

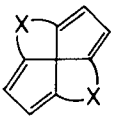

19a X = $-(CH_2)_2-$
b X = –CH=CH–

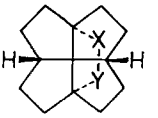

20a X = Y = CH_2
b X = O, Y = CO

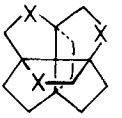

21a X = CH_2
b X = O

---

[4]) Fenestranes are spiroalkanes, in which two polymethylene bridges connect each of the α,α′ -positions between the spiro rings.

[5]) *Fischer* projections are used throughout for the configuration of the central $C(C)_4$ entity in fenestranes; formula **12** represents the absolute configuration of this compound.

[6]) This also applies to derivatives of [4.4.5.5]- and [4.4.4.5]fenestranes [9] [10][2]). We thank Prof. *W. G. Dauben* and Prof. *W. C. Agosta* for communicating crystal-structure data prior to publication.

[7]) The 6 stereoisomers differ in the number of *cis*- and *trans*-fused subunits of bicyclo[3.3.0]octane [3]. According to IUPAC nomenclature all-*cis*-[5.5.5.5]fenestrane (**14a**) is *cis-transoid-cis-transoid-cis-transoid-cis-transoid*-tetracyclo[5.5.1.$0^{4,13}$.$0^{10,13}$]tridecane and *c(is), c(is), t(rans), t(rans)*-[5.5.5.5]fenestrane **15** is *cis-cisoid-cis-transoid-trans-cisoid-trans-transoid*-tetracyclo[5.5.1.$0^{4,13}$.$0^{10,13}$]tridecane.

[8]) The synthesis of all-*cis*-[5.5.5.5]fenestrane has been reported in [11].

fused structural entities of bicyclo[3.3.0]octane, opposite bond angles of the central $C(C)_4$ fragment are opened, leading to substantial s_{2a} vectors *(Appendix 1)* and planarization indices [4] *(cf. Table 1)*. Planoid distortions in fenestranes are also enhanced by bridgehead substitution. The parent molecule **14a** has a planarization index [4] $P_C = 0.089$, whereas its tetramethyl-substituted counterpart **14b** has $P_C = 0.18$. This is due almost exclusively to an increase of the $s_{2a}(E)$ vector, the small $s_{2b}(E)$ contribution being unaffected (**14b**: $s_{2a} = 18.79°$, $s_{2b} = 0.025°$). These results suggest that planoid distortions in fenestranes might, in general, depend on the size of bridgehead substituents. Peripheral double bonds may also enhance planoid distortions in fenestranes *viz.* P_C(**14a**) = 0.089, P_C(**16**) = 0.13. A shift of one double bond in **16**[9]) to the bridgehead position yields **17**, P_C increases from 0.13 to 0.21. This tendency is enhanced considerably in **18**, which contains four bridgehead double bonds and which, according to our MNDO results, contains two opposite bond angles of 139.6°, leading to a $P_C = 0.47$ for this compound. The local structure of the $C(C)_4$ moiety in the annullene with the central C-atom, **19b**, has a bond angle deformation vector $s_{2a} = 49.4°$ and a $P_C = 0.48$, very similar to that of the tetraene **18**. Contrary to **14b** with bridgehead CH_3 groups ($s_{2a} = 18.79°$, $s_{2b} = 0.025°$), the centropentaquinane **20a**, which is a fenestrane with one additional ethylene bridge, shows quite normal bond angles and hence small planoid deformations in the central $C(C)_4$ fragment ($s_{2a} = 4.78°$, $s_{2b} = 0.09°$); its planarization index is very similar to that of **13**[10]). For the centrohexaquinane **21a**[11]) [5], which contains three interwoven spiro[4.4]nonane subunits and hence qualifies as a bridged [5.5.5.5]fenestrane, a completely undistorted $C(C)_4$ substructure with $s_{2a} = s_{2b} = 0°$ and $P_C = 0$ has been found. Thus, **21a** as yet unprepared is one of the few more complex compounds, which contains a quaternary C-atom with an ideal tetrahedral configuration.

Evaluation of Strain. – To assess the stability of the [5.5.5.5]fenestranes discussed above, the strain energies have been estimated. Because of the lack of thermochemical data, MNDO results [8] have been used (*Tables 1* and *2*).

Particularly noteworthy are the stereoisomers of the [5.5.5.5]fenestranes of type **II** (*Fig. 1*, $m = n = 2$). With increasing compression, the strain energy increases consid-

Table 1. *Planarization Indices, Heats of Formation, and Strain Energies in the Stereoisomeric [5.5.5.5]Fenestranes*

[5.5.5.5]Fenestrane ring fusions[a])	Symmetry	Planarization index P_C [4]	Heat of formation[b]) [kJ/mol]	Strain energy[c]) [kJ/mol]
cccc (**14a**)	D_{2d}	0.089	–171.2	0
ccct	C_s	0.248	–81.2	90.0
ctct	C_v	0.43	94.89	266.1
cctt (**15**)	C_2	0.467	138.5	309.7
cttt	C_s	0.70	377.98	549.2
tttt	D_{2d}	0.98	591.3	762.5

[a]) *c(is)* and *t(rans)* refer to the fused subunits of bicyclo[3.3.0]octane[7]).
[b]) MNDO results.
[c]) With *cccc*-[5.5.5.5]fenestrane (**14a**) as reference point.

[9]) Tetraene **16** has recently been prepared [12].
[10]) For the synthesis of the fenestrane-carbolactone **20b**, see [3].
[11]) Synthesis of the trioxyderivative **21b** have been reported [13a, b].

Table 2. *Planarization Indices* P_C, *Heats of Formation, and Strain Energies of the [5.5.5.5] Fenestranes* **13–20a** *and* **21a**

Structure	Planarization index P_C [4]	Heat of formation[a] [kJ/mol]	Strain energy [kJ/mol]
13	0.082	–613.9	27[b]
14a	0.089	171.2	23[b]
14b	0.18	18.8	353[b]
15	0.47	138.53	332.7[b]
16	0.13	295.01	35[b]
17	0.21	314.8	19.8[c][d]
18	0.47	471.7	176.7[c]
19a	0.43	446.76	151.8[c]
20a	0.05	–146.13	70.0[b]
21a	0.0	–119.99	128[b]

[a]) MNDO results.
[b]) Estimated by comparison with the sum of group parameters [14].
[c]) Relative to compound **16**.
[d]) π-Delocalisation not included.

erably. On the reasonable assumption, that the major contribution to the strain is due to bond-angle and bond-lengths deformations in the central $C(C)_4$ fragment[12]), the local strain energy becomes very large. Whether the highly strained isomers would release part of the strain by isomerization to the more stable isomers *via* cleavage of one bond is at present a matter of a speculation. Comparison of the tetraenes **16–19a** with each other *(Table 2)* reveals, that introduction of bridgehead double bonds also leads to an increase in strain. Since P_C of **19b** is very similar to that found for **19a** and the tetraene **18**, and since twist distortions are essentially absent in the central $C(C)_4$ fragment, it may be concluded, that the local strain in these three molecules is very similar.

On the basis of comparison of the MNDO energy of **14a** and **16** with the heat of formation estimated by group parameters [14], the overall strain in these two molecules appears to be rather small *(Table 2)*. Moderate strain is indicated for **20a** and **21a** by a similar evaluation.

In view of the planarization indices for **20a** and **21a** (P_C(**20a**) = 0.046, P_C(**21a**) = 0), it is clear that is not a general parameter for strain in fenestranes. It is a structural index for describing planoid distortions rather than a parameter for local strain of $C(C)_4$ fragments in spiro compounds. It might be used for evaluation of local strain only in those cases, where the s_{2b} contribution to the overall deformation of the $C(C)_4$ fragment is similar or negligible (see below). The experimental verification of the structural and energetic MNDO results has to await the synthesis of the more highly strained fenestranes[13]).

Further Aspects of Energy. – Since distortions affect bond angles as well as bond lengths, their possible interdependence was of particular interest. The plots $S_3(T_2)$ *vs.* $S_4(T_2)$ *(Fig. 4a)* and $S_1(A_1)$ *vs.* $S_2(E)$ *(Fig. 4b)* clearly show that these two vectors are

[12]) The internal bond lengths increase from 157 pm in the *cccc*-isomer **14a** to 164 pm in the *tttt*-isomer[7]), whereas the changes in the external bonds are smaller than ±1.5 pm.
[13]) For attempts to prepare the *cccc*-isomer of [5.5.5.5]fenestrane, see [15].

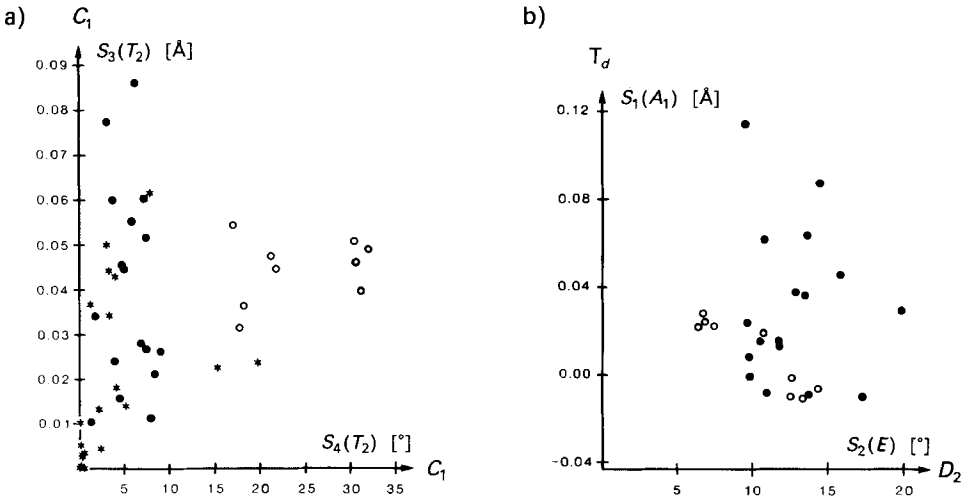

Fig. 4. *Bond-length* [pm] vs. *bond-angle* [°] *deformations for the central* $C(C)_4$ *fragment of spiro[4.4]nonanes of type* **I** *and* **II** (*Fig. 1*). a) $S_3(T_2)$ *vs.* $S_4(T_2)$; linear regression: $s_3(T_2)$ [pm] = 0.000344 (±0.00037) $s_4(T_2)$[°] + 0.0362 (+0.0058), $R = 0.182$. b) $S_1(A_1)$ *vs.* $S_2(E)$, only crystal-structure data are shown; linear regression: $s_1(A_1)$[pm] = −0.00050 (±0.00201) $s_2(E)$[°] + 0.0281 (±0.0245), $R = 0.05$. *: MNDO Data; ●: crystal structure data; ○: structures with $s_2(E) < s_4(T_2)$.

independent of each other in the range of $s_2(E) < 20°$[14])[15]). This result might have been expected: in an attempt to derive features of the potential energy hypersurface, *Dunitz* and coworkers have discussed the implications of the deformation vectors for the energy on the basis of a quadratic approximation to the potential energy [17]. They clearly stated that cross-terms between two coordinate that transform as different irreducible representations have to be identical zero, as long as the quadratic approximation for the potential energy holds. It was further stated, that a quadratic approximation cannot be expected to hold for large deformations from the T_d reference symmetry. Since no crystal structures of spiro compounds have yet been reported with deformations large enough for detection of this feature, MNDO-structural data of the stereoisomeric [5.5.5.5]-fenestranes have been analyzed for the possible interdependence of their $s_1(A_1)$ and $s_2(E)$ vectors (*Fig. 5*). It is apparent that large planoid bond-angle deformations lead to increasing bond lengths. If the large distortions from T_d symmetry are described correctly by MNDO calculations, it may also be concluded, that a non-linear correlation between bond-length and bond-angle deformations does exist.

In addition, MM2 results [18] for the same six stereoisomers of the [5.5.5.5]fenestrane have been analyzed in the same manner (*Fig. 5*). The interdependence of bond-angle ($S_2(E)$) and bond-length deformations ($S_1(A_1)$) are quite different from the MNDO correlation. Apart from the rather small changes in bond lengths with increasing $s_2(E)$

---

[14]) We have verified that this conclusion is independent of whether the quaternary C-atom in these [5.5.5.5]fenestranes is bonded to saturated or unsaturated C-substituents.

[15]) An estimate of the average molecular dimensions of the central $C(C)_4$ fragments in the six compounds for which experimental standard deviations had been available, has shown, that environmental can be detected [16]: for bond angles, $\bar{x}_u = 109.33°$ ($\sigma(\bar{x}_u) = 1.90°$), σ^2(sample) = 29.04, $\sigma^2(x_i) = 54.38$, and $\chi^2 = 148\,076$; for bond lengths, $\bar{x}_u = 1.551$ Å, ($\sigma(\bar{x}_u) = 0.034$ Å), σ^2(sample) = 0.00898, $\sigma^2(x_i) = 0.0054$, and $\chi^2 = 1592$.

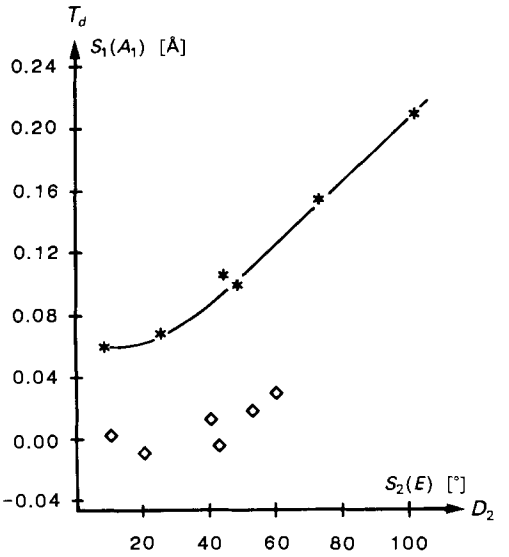

Fig. 5. *Bond-length* ($S_1(A_1)$) vs. *bond-angle* ($S_2(E)$) *deformations for the stereoisomeric [5.5.5.5]fenestranes* (*cf. Table 1*). *: MNDO Data; ◇: MM2 data.

vector, the MM2 results indicate much smaller planoid distortions. This underlines the well known fact, that force fields, used for strain energy calculations, are in general not parametrized for large distortions. Based on our limited results, MM2 structures may only be reliable for bond-angle deformations $s_2(E) < 20°$.

The central $C(C)_4$ fragments of spiro compounds with a spiro[4.4]nonane substructure show a wide range of different bond-angle deformations (see also Fig. 3 and 4 in [4]). These distortions are due to specific structural features of peripheral groups in these polycyclic molecules. Nevertheless, it is of interest, which type of deformation a molecule like CH_4 would prefer, if it would have options for different types of planoid distortions. For this purpose, some *ab-initio* calculations (6-31G) [19] have been performed for distorted CH_4 with $s_2(E)$ bond-angle vectors fixed at 20°, 40°, and 60°. Since both the $s_{2a}(E)$ and the $s_{2b}(E)$ vectors contribute to the $s_2(E)$ bond-angle distortion vector, the deformations have been chosen in such a way, that the $s_2(E)$ vector coincides with either the S_{2a} or the S_{2b} axis (*cf. Fig. 3*). For the same $s_2(E)$ bond-angle deformation vector, the strain is smallest for values $s_{2a} < 0$ and highest along the S_{2a} coordinate ($s_{2a} > 0$). This trend is related to a similar increase in nuclear repulsion (*Fig. 6*) and suggests that planoid deformations follow preferentially the lowest nuclear repulsion[16]). If an extrapolation to the central $C(C)_4$ fragments in bi- and polycyclic molecules containing spiro[4.4]nonane subunits is possible, the wide range of bond-angle deformations found in the region between the S_{2a} and the S_{2b} axis (*cf.* [4]) is not surprising. This also suggests that the molecular constraints in [5.5.5.5]fenestranes like **14** or **15** are such, that the nuclear repulsions in the central $C(C)_4$ moieties are larger than in spiro structures with polymethylene bridges in α,β'- or β,β'-positions.

[16]) Quantum-chemical calculations for CH_4 distorted according to the symmetry-deformation coordinate $S_{2a}(E)$ (*Fig. 1*), eventually leading to the planar configuration, have been reported and discussed by *Wiberg et al.* [20].

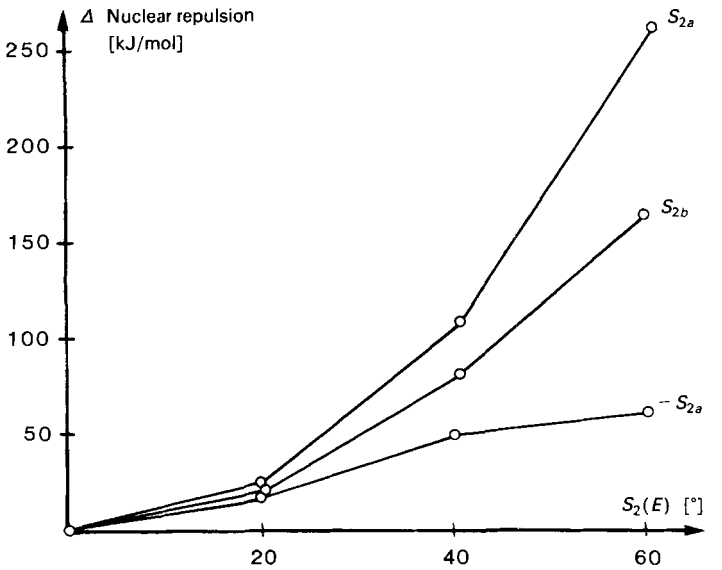

Fig. 6. *Distortion of CH_4 along the S_{2a}, S_{2b}, and $-S_{2a}$ symmetry-deformation coordinate* [4]. Nuclear repulsion relative to CH_4 with T_d symmetry [kJ/mol] *vs.* $S_2(E)$ [°].

Conclusions. – Most of the crystalline spiro[4.4]nonanes with one polymethylene bridge between the α,α'-positions of the two rings (type **I**, *Fig. 1*) have $s_2(E)$ deformation vectors, which are dominated by S_{2a}-type distortions. C_{2v}-Type distortions increase in these molecules, if the polymethylene bridge becomes shorter. The planoid S_{2a}-type deformations in the structures investigated are more pronounced than in corresponding spiro compounds, which have polymethylene bridges only in α,β'- or β,β'-positions [4]. In crystal as well as MNDO structures of fenestranes, which are derived from spiro-[4.4]nonane (*Fig. 1*, type **II**), two large opposite bond angles are found. They give rise to $s_2(E)$ bond-angle distortion vectors, which in most cases coincide with the S_{2a} coordinate. This unusual class of compounds, which is under active exploration in several laboratories [3] [8–11] [21] certainly deserves special attention, because it provides a direct entry into compounds with significant planoid distortions.

Appendix. – *Identification of Structures Analyzed* (*Fig. 1*). The structures are listed according to their *CAS*-registry numbers, *Cambridge Datafile* identifiers $s_{2a}(E)$, $s_{2b}(E)$, and $s_4(T_2)$ deformation vectors. a) *X-Ray Structures.* [40184-99-4] RETIGB10 (**1a**) 12.99, 4.50, 3.808; [65400-02-4] ISCOMD (**2**) 9.385, 5.551, 5.963; [74806-72-7] DOPHBL10 (**3**) 8.149, 5.042, 6.291 and 13.730, 4.798, 3.199; [80246-78-2] BAJRIN10 (**4**) 8.970, 6.305, 5.072; [34416-71-2] HSDAPH (**5**) 6.928, 7.00, 7.372; [80151-96-8] BECKOJ (**6**) 9.324, 5.05, 6.883; [76652-56-7] DODECC (**7**) 10.077, 7.693, 17.127; [71729-53-8] CABGAN (**8**) 14.261, 2.20, 21.334; [89702-41-0] CAYVUU (**9**) 7.021, 0.916, 32.337 and 7.127, 0.207, 31.196 and 7.629, 0.035, 30.669 and 6.671, 1.405, 32.059; [60221-50-3] TCPMNE (**10**) 22.26, 19.35, 41.48 ($R > 0.1$); [23109-14-0] (**11a**) 15.167, 8.50, 1.036; [23012-56-8] (**11b**) 18.937, 6.00, 0.00; [79076-84-9] POPATC (**11c**) 7.130, 11.95, 4.573; [72062-13-6] BLAREN (**12a**) 15.358, 4.30, 7.238; [67490-04-4] BEHZIX (**13**) 11.836, 0.30, 1.839; [56547-94-5] DXIFPO 9.959, 6.35, 8.022; [78046-18-1] BEHZOD 8.372, 5.30, 8.503 and 8.487, 5.0, 7.509; [82447-37-8] BEWNIA 10.306, 8.85, 9.144; [82439-63-2] BEWNOG 10.479, 2.65, 21.876; [80246-71-3] BAJRIN 9.070, 6.33, 4.890; [87638-02-6] CEFLII 12.533, 3.382, 4.589; [76652-57-8] DODECB 10.516, 7.009, 17.770 and 11.050, 7.616, 18.246.

b) *MNDO Structures* (without *CAS*-registry numbers). **12b:** 15.317, 5.58, 7.95; **13:** 8.551, 0.10, 0.064; **14a:** 9.311, 0.010, 0.048; **14b:** 18.79, 0.025, 0.432; **15:** 48.598, 3.746, 2.198; **16:** 13.545, 0.0, 0.137, **17:** 21.817, 0.046, 4.091; **18:** 49.00, 0.0, 0.004; **19a:** 44.92, 2.15, 2.418; **19b:** 49.424, 1.027, 0.527; **20a:** 4.78, 0.09, 4.30; **21a:** 0.0, 0.002, 0.011.

This work is supported by the *Swiss National Science Foundation* (project No. 2.421-0.82 and 2.236-0.84).

REFERENCES

[1] a) R. Hoffman, R.W. Alder, C.F. Wilcott, Jr., *J. Am. Chem. Soc.* **1970,** *92,* 4992; R. Hoffman, *Pure Appl. Chem.* **1971,** *28,* 181; b) M.C. Boehm, R. Gleiter, P. Schang, *Tetrahedron Lett.* **1979,** 2575; c) J. Chandrasekhar, E.-U. Würthwein, P.v.R. Schleyer, *Tetrahedron* **1981,** *37,* 921.

[2] a) R. Keese, A. Pfenninger, A. Roesle, *Helv. Chim. Acta* **1979,** *62,* 326; b) R. Keese, *Nachr. Chem. Techn. Lab.* **1982,** *30,* 844; c) E.-U. Würthwein, J. Chandrasekhar, E.D. Jemmis, P.v.R. Schleyer, *Tetrahedron Lett.* **1981,** *22,* 843.

[3] A. Pfenninger, R. Roesle, R. Keese, *Helv. Chim. Acta* **1985,** *68,* 493.

[4] W. Luef, R. Keese, H.-B. Bürgi, *Helv. Chim. Acta* **1987,** *70,* 534.

[5] P. Gund, T. Gund, *J. Am. Chem. Soc.* **1981,** *103,* 4458.

[6] W. Luef, R. Keese, manuscript in preparation.

[7] F.H. Allen, S. Bellard, M.D. Brice, B.A. Carthwright, A. Doublenday, H. Higgs, T. Hummelink, B.G. Peters, O. Kennard, W.D.S. Motherwell, J.R. Rodgers, D.G. Watson, *Acta Crystallogr., Sect. B* **1979,** *35,* 2331.

[8] M.J.S. Dewar, W. Thiel, *J. Am. Chem. Soc.* **1977,** *99,* 4899; QCPE No. 353.

[9] W.G. Dauben, D.M. Walker, *Tetrahedron Lett.* **1982,** *23,* 711.

[10] a) V.B. Rao, S. Wolff, W.C. Agosta, *J. Chem. Soc., Chem. Commun.* **1984,** 293; b) V.B. Rao, C.F. George, S. Wolff, W.C. Agosta. *J. Am. Chem. Soc.* **1985,** *107,* 5732.

[11] a) M. Luyten, R. Keese, *Angew. Chem.* **1984,** 96, 356; *ibid Int. Ed.* **1984,** *23,* 390; b) M. Luyten, R. Keese, *Helv. Chim. Acta* **1984,** *67,* 2242.

[12] M. Desphande, G. Kubiak, M. Jawdosiuk, U. Weiss, J.M. Cook, *J. Am. Chem. Soc.* **1985,** *107,* 4786.

[13] a) H.E. Simmons III, J.E. Maggio, *Tetrahedron Lett.* **1981,** *22,* 4456; b) L.A. Paquette, M. Vazeux, *Tetrahedron Lett.* **1981,** *22,* 291.

[14] J.D. Cox, G. Pilcher, 'Thermochemistry of Organic and Organometallic Compounds', Academic Press, London, 1970, p. 590.

[15] M. Luyten, R. Keese, *Tetrahedron* **1986,** *42,* 1687.

[16] R. Taylor, O. Kennard, *Acta Crystallogr., Sect. B* **1983,** *39,* 517.

[17] P. Murray-Rust, H.B. Bürgi, J.D. Dunitz, *Acta Crystallogr., Sect. B* **1978,** *34,* 1793.

[18] U. Burkert, N.L. Allinger, Molecular Mechanics, ACS Monograph 177, Am. Chem. Soc., Washington, D.C., 1982; QCPE No. 395.

[19] W.G. Richards, D.L. Cooper, 'ab initio Molecular Orbital Calculations for Chemistry', 2nd edn., Oxford University Press, Oxford, 1983; Gaussian 80, QCPE No. 437.

[20] a) K.B. Wiberg, G.B. Ellison, J.J. Wendoloski, *Tetrahedron* **1974,** *30,* 1573; b) K.B. Wiberg, G.B. Ellison, J.J. Wendoloski, *J. Am. Chem. Soc.* **1976,** *98,* 1212.

[21] M.T. Crimmins, S.W. Mascarella, L.D. Bredon, *Tetrahedron Lett.* **1985,** *26,* 997.